Polymer Bulletin (2024) 81:7481–7497
https://doi.org/10.1007/s00289-023-05054-3

ORIGINAL PAPER

Amino-terminated hyperbranched poly(phenylene oxide) as a novel antioxidant for nitrile-butadiene rubber

Heba Kandil[1] · A. A. Ward[2] · T. A. Zidan[1]

Received: 4 August 2023 / Revised: 29 October 2023 / Accepted: 30 October 2023 /
Published online: 27 November 2023

Abstract

Amino-terminated hyperbranched poly(phenylene oxide), (APO) is evaluated as a novel antioxidant for nitrile-butadiene rubber (NBR). By using a two-roll mill, APO was incorporated into NBR mixes at two different concentrations: 1 & 2 phr. The cure characteristics, physico-mechanical, thermal and dielectric properties of the prepared NBR vulcanizates are evaluated. The NBR vulcanizates underwent thermo-oxidative aging, and subsequently, the assessment of their retained physico-mechanical properties was conducted. The prepared NBR vulcanizates with 1 phr of APO show high antioxidant efficiency as the commercial *N*-isopropyl-*N*′-phenyl-*p*-phenylene-diamine (IPPD). The dielectric results show a decrease in permittivity, dielectric loss and conductivity with the addition of APO. The findings of this study demonstrate the potential utility of NBR vulcanizates containing 1 phr of APO for applications demanding improved dielectric properties, mechanical durability, thermal stability, and resistance to degradation such as electrical insulation in power distribution systems, capacitor manufacturing, automotive parts, and industrial machinery.

Keywords Poly(phenylene oxide) · Nitrile-butadiene rubber · Antioxidant · Physico-mechanical properties · Dielectric properties

Introduction

Acrylonitrile–butadiene rubber (NBR) is a versatile synthetic rubber that plays a crucial role in various industries. Its unique properties, such as oil resistance, flexibility, durability and electrical insulation, make it an indispensable material for numerous

✉ T. A. Zidan
tayseerzidan@yahoo.com

[1] Department of Polymers and Pigments, National Research Centre, Dokki, Giza 12622, Egypt

[2] Microwave Physics and Dielectrics Department, National Research Centre, Dokki, Giza 12622, Egypt

applications such as automotive, aerospace, oil and gas, construction, medical, food and electronic industries [1–6]. Despite its remarkable properties, NBR is not impervious to the degrading effects of the environment [7]. When exposed to factors such as heat, oxygen, ozone, and ultraviolet, NBR can undergo degradation processes, leading to a reduction in its performance and service life [7]. So, antioxidants are added to NBR products to protect it from degradation caused by environmental factors [8–10]. Commonly, low molecular weight antioxidants have been widely utilized in rubbers to inhibit degradation [10–12]. However, these antioxidants come with certain limitations that have promoted researchers and industries to seek for alternative antioxidants. One of the disadvantages of these materials is their tendencies to volatilize and migrate to the surface of the rubber due to their small weights, which causes their low effectiveness in preventing oxidation and extending the life of rubber products [11, 13]. To overcome this problem, several methods have been developed [11, 13, 14], one of which is by the addition of polymeric antioxidants. There are two methods of preparing polymeric antioxidants. The first approach involves synthesizing polymeric antioxidant with a functional monomer having antioxidant properties, while the second one involves binding low molecular weight antioxidants to the polymer chains [13]. Traditionally, linear polymeric antioxidants have been extensively studied. However, an increasing attention has been paid recently to a class of polymers known as hyperbranched polymers (HPs) as potential antioxidants [13, 15]. HPs are polymers that possess a highly branched, three dimensional structure with multiple reactive groups, providing unique advantages over their linear counterparts [16]. The interest in HPs stems from their highly branched structure providing a significantly higher number of reactive sites resulting in more opportunities for antioxidant reactions, enabling them to scavenge free radical and reactive oxygen species more effectively [15, 16].

Accordingly, we are interested here in investigating the thermo-oxidative aging resistance of hyperbranched poly(phenylene oxide) for NBR compounds. Hyperbranched poly(phenylene oxide) terminated with amino group (APO) was prepared for the first time in our previous work via one-pot polymerization reaction between 4-chloro 2-amino phenol and phloroglucinol [17], and its antioxidant activity was not studied yet. Hence, it was incorporated into NBR compounds here at two different loadings to study its antioxidant activity and for comparing, commercial antioxidant IPPD was used. In addition, its effect on the cure characteristics, physico-mechanical, thermal and dielectric properties of the prepared NBR vulcanizates is studied in detail. The NBR vulcanizates were exposed to thermo-oxidative aging to evaluate their retained physico-mechanical properties.

Experimental

Materials

Amino-terminated hyperbranched poly(phenylene oxide); APO was synthesized in a previous work [17]. It is crystalline powder with black color. Its particle size is in the range of 22.38–23.32 nm. Acrylonitrile–butadiene rubber (NBR) with a specific

Table 1 Formulations for the preparation of NBR compounds

Ingredients (phr)	NBR compounds code			
	N (blank)	NC	NP1	NP2
NBR	100	100	100	100
ZnO	5	5	5	5
Stearic acid	2	2	2	2
Silica	50	50	50	50
IPPD	–	1	–	–
APO	–	–	1	2
CBS	3	3	3	3
S	1	1	1	1

Table 2 The cure characteristics of the NBR compounds

Compound code	N	NC	NP1	NP2
$M_H - M_L$	15.2	15.47	15.54	15.35
Ts_2	1	0.9	1.3	0.9
Tc_{90}	13.50	12.19	13.95	12.25
CRI	8	8.9	7.9	8.8

gravity of 1.17 ± 0.005 and a 32% acrylonitrile content was purchased from Bayer AG in Germany. Stearic acid (St. Ac) and zinc oxide (ZnO) with specific gravity 0.9–0.97 and 5.55–5.61, respectively, at 15 °C were used as activators. Silica with surface area 150 ± 25 m^2/g and an average particle size of 15 nm was used as reinforcement agent. *N*-isopropyl-*N*′-phenyl-*p*-phenylene-diamine (IPPD) was used as commercial antioxidant. *N*-cyclohexyl-2-benzothiazole sulfenamide (CBS), pale gray powder, specific gravity of 1.27–1.31 at room temperature (25 °C ± 1), melting point 95–100 °C was used as an accelerator. Elemental sulfur, fine pale-yellow powder, specific gravity of 2.04–2.06 at room temperature was used as vulcanizing agent. All chemicals were supplied by Sigma-Aldrich, Germany.

Preparation of NBR compounds

To prepare NBR compounds, NBR was combined with other ingredients on a two-roll mill. The ingredients were incorporated in the order listed in Table 1. In a hydraulic press set at 152 °C, the NBR compounds were vulcanized at the time (TC_{90}) obtained from rheometric characteristics in Table 2 at "Cure characteristics" section. under pressure of approximately 4 MPa/cm^2.

APO is related to the prepared star-shaped hyperbranched poly(phenylene oxide) with terminal amino groups. N, NC, NP1 and NP2 are related to blank NBR compound, NBR compound with commercial IPPD, NBR compounds with APO at two different concentrations: 1 & 2 phr, respectively.

Characterization and tests

Cure characteristics

A Monsanto Moving Die Rheometer (MDR 2000) was used to measure the cure characteristics of NBR compounds in accordance with ASTM 2084–95. The cure characteristics that were measured involve the torque difference ($M_H - M_L$), the scorch time (ts_2), and the optimum cure time (tc_{90}) while the cure rate index (CRI) was calculated using the following formula,

$$\mathrm{CRI} = 100/\left(tc_{90} - ts_2\right)$$

Cross-link density

Cross-link density was determined using the equilibrium swelling method according to the previous report [10] where 0.1–0.2 g of each compound sample was weighed and then immersed in toluene-filled closed bottles for 24 h at 25 °C until they reached an equilibrium swelling state. Subsequently, the swollen specimen was removed, its surface rapidly wiped, and its weight measured to express the change as the swelling percentage.

$$Q\% = \frac{\text{Swollen weight} - \text{Original weight}}{\text{Original weight}} \times 100$$

To determine the molecular weight between cross-links (Mc in g/mol), the Flory–Rehner equation was applied.

$$M_c = \frac{-\rho V s V_r^{\frac{1}{3}}}{\left[\mathrm{In}\left(1 - V_r\right) + V_r + \chi V_r^2\right]}$$

In this equation, ρ represents the density of NBR rubber (1.17 g/cm^3) while Vs is the molar volume of toluene (106.3 ml/mol), V_r is the volume fraction of swollen rubber, and χ represents the interaction parameter of the rubber network and solvent (χ of NBR = 0.39). Vr was calculated based on swelling data using the following equation,

$$V_r = \frac{W_r/\rho_1}{W_r/\rho_1 + W_s/\rho_0}$$

Wr and Ws represent the weight of the swollen NBR rubber and toluene, while ρ_1 and ρ_0 represent NBR density (1.17 g/cm^3) and solvent density (0.867 g/cm^3 for toluene).

Once the molecular weight between cross-links (Mc) was determined, the degree of cross-linking (υ; mol/cc) could be then calculated using the equation:

$$\upsilon = 1/\left(2M_c\right)$$

For each compound, three samples were tested independently.

Physico-mechanical properties

Mechanical properties of the produced vulcainzates were determined according to ASTM D 412-15a, in which the mechanical properties of the vulcanizates were evaluated on a Zwick tensile testing machine (1425; Germany) at a crosshead speed of 500 mm/min and at room temperature. Hardness (Shore A) for the produced vulcainzates was measured according to ASTMD2240-15 using Bareiss Shore A (Oberdischingen, Germany).

Thermo-oxidative aging test

For thermo-oxidative aging test, the vulcanizates were subjected to thermo-oxidative aging in an electric oven at 90 °C for various times: 2, 4 and 6 days, according to ASTM D573-04. The rubber's retained physico-mechanical properties were compared to those of a rubber that also contained a conventional antioxidant IPPD.

Retention in tensile properties was calculated as follows:

$$\text{Retention } (\%) = \frac{\text{Value after aging}}{\text{Value before aging}} \times 100$$

Thermogravimetric analysis

A thermogravimetric analyzer (TGA-50 Shimadzu) with a temperature range of 25–600 °C was used to determine the thermal stability of NBR compounds at a heating rate of 10 °C/min under a nitrogen atmosphere.

Dielectric spectroscopy technique

By using a high-resolution broadband impedance analyzer (Schlumberger Solartron 1260), an electrometer, amplifier, and measuring cell, dielectric and conductivity measurements were made. The AC electric field was applied with a frequency range of 0.1 Hz to 1 MHz. The error in dielectric loss ε'' and permittivity ε' is equal to 1% and 3%, respectively. A temperature regulator with a Pt 100 sensor was used to regulate the samples' temperature. The measurement error for temperature is 0.5 °C. The samples were kept in desiccators with silica gel to prevent moisture. Following that, the sample was moved to the measuring cell and kept there with P_2O_5 until the measurements were made.

Results and discussion

A novel antioxidant for nitrile-butadiene rubber (NBR), APO, was synthesized from nucleophilic substitution reactions between 4-chloro-2-amino phenol and phloroglucinol according to the previous report [17]. Its structure is represented in Fig. 1. To study its antioxidant activity in rubber compounds, it was mixed with NBR compound at two different concentrations. The cure characteristics, mechanical, antiaging, and dielectric properties of the NBR compounds prepared with and without APO were investigated in detail, and for comparing IPPD, a commercial antioxidant was used.

Cure characteristics

A Monsanto Moving Die Rheometer was used to measure the produced NBR compounds' cure characteristics at 152 °C for 30 min, and the results are shown in Table 2.

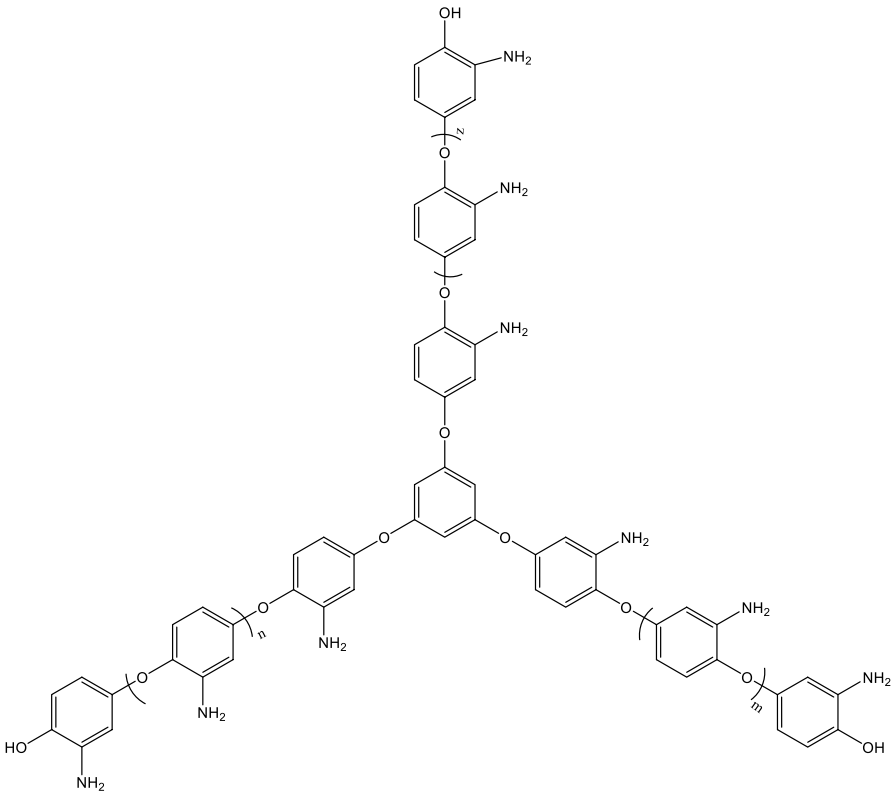

Fig. 1 Chemical structure of amino-terminated hyperbranched poly(phenylene oxide)

According to the present data, it was found that the investigated APO has a slight impact on the cure characteristics of the NBR compound as compared to the blank and that prepared with IPPD. Moreover, it was found that with increasing the APO concentration above 1 phr, the scorch time (ts_2) and the optimum cure time (Tc_{90}) are reduced while the curing rate index (CRI) is increased. The decrease in the value of Tc_{90} & ts_2 and the increase in the value of CRI indicates that APO has an accelerating effect and this may be attributed to increasing the amine contents that accelerates the vulcanization rate [18, 19]. Furthermore, it was observed that the torque difference ($M_H - M_L$) which is an indication of the degree of cross-link density within rubber compound was slightly increased by the addition of 1 phr of APO compared to that of blank NBR compound (N) and was similar to that prepared from commercial IPPD (NC). However, with the addition of 2 phr of APO, a slight decrease in $M_H - M_L$ was observed. This indicates that the value of cross-link density increases by adding 1 phr of APO and decreases beyond using 1 phr. This result is discussed further in the next section "Cross-link density".

Cross-link density

Equilibrium swelling (%) and cross-link density of NBR compounds with and without APO were evaluated using swelling test in toluene for 24 h and the results are displayed in Fig. 2. The results demonstrated that the addition of 1 phr of APO increases the cross-link density of NBR compounds. This enhancement is attributed to the presence of amino groups in APO which chemically activates both rubber chains and elemental sulfur during curing reactions by formation of intermediate complexes with the other rubber curatives. Consequently, the available elemental sulfur becomes more efficiently linked to the rubber chains, resulting in higher degree of cross-links [19].

The addition of 2 phr of APO shows a decrease in the value of cross-link density. This decrease may be attributed to the presence of an excessive amount of APO in the NBR, which may be present in the form of layers within the rubber compound that prevented the rubber chains from interacting with silica [18]. As a result, the cross-link density decreased.

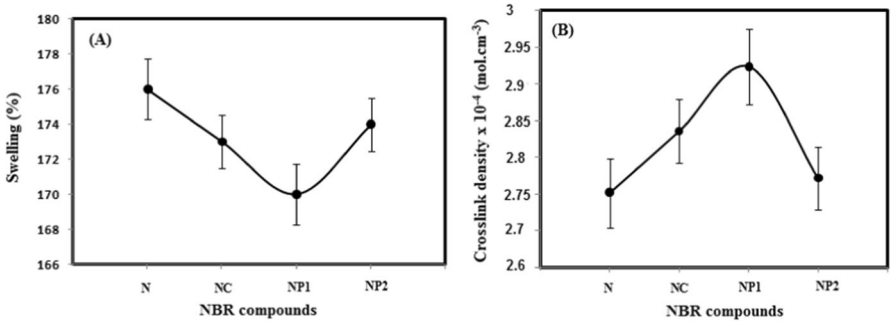

Fig. 2 Equilibrium swelling % **A** and cross-link density **B** of NBR without antioxidant (N), NBR with commercial IPPD (NC), NBR containing 1 phr of APO (NP1) and NBR containing 2 phr of APO (NP2)

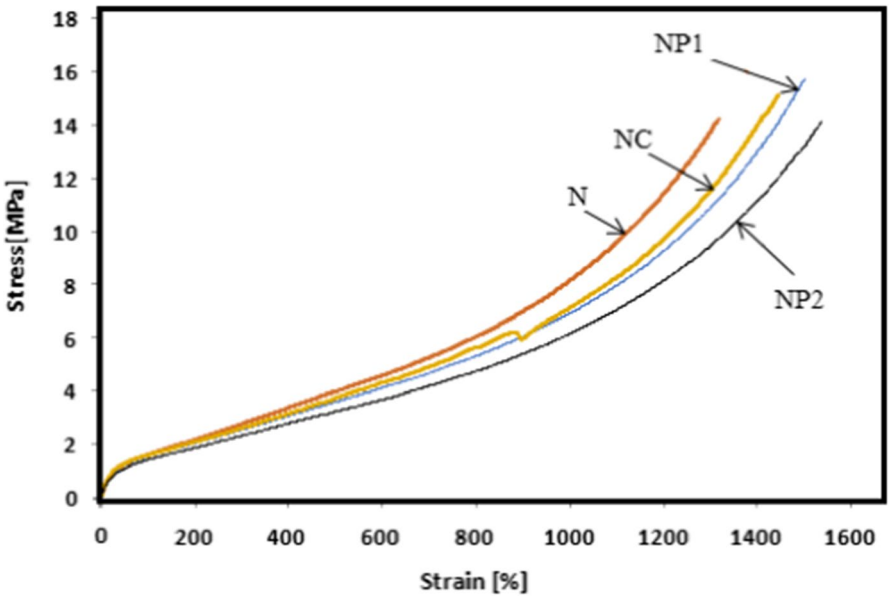

Fig. 3 Stress–strain curves of the prepared NBR compounds

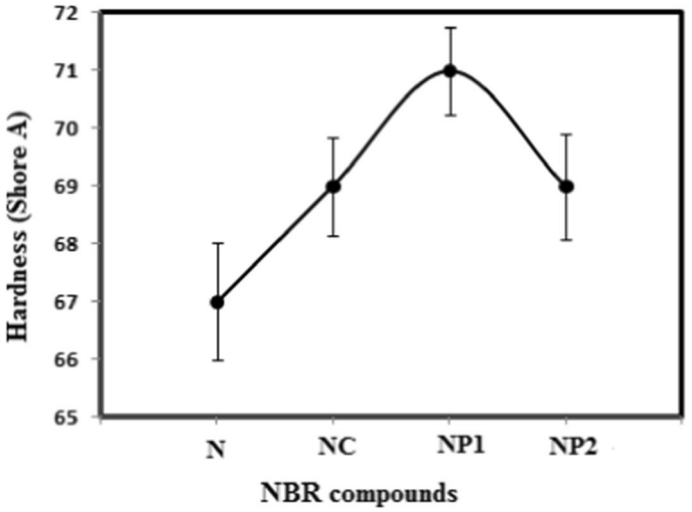

Fig. 4 Hardness of the prepared NBR compounds

Physico-mechanical properties

Figures 3 and 4 display the stress–strain curves and hardness of the prepared NBR compounds, respectively. As shown, the compounds containing APO either 1 or 2 phr show an observed improvement in their physico-mechanical properties (stress,

strain, and hardness) as compared with the blank and that contain commercial IPPD in its formulation. This improvement was due to increased cross-link density [20]. Moreover, it is observed that the result of using 1 phr of APO is almost similar to that prepared from commercial IPPD (NC), but increasing the concentration of APO beyond 1 phr, results in a slight decrease in the mechanical properties. This decrease is attributed to the low decrease in the cross-link density as explained before. It seems that adding 1 phr of APO in rubber mixes is the optimum concentration for producing compound with superior quality.

Thermo-oxidative properties

The prepared NBR compounds underwent thermo-oxidative aging for various periods of time, up to six days, in an oven set at 90 °C. Figures 5 and 6 display the results of aging. The data presented shows that as the number of aging days increases, the retention rates of mechanical parameters such as tensile strength and elongation at break of NBR compounds decline.

In comparison with blank samples, commercial NBR compounds (IPPD) and compounds containing APO degrade rather slowly over time, demonstrating that the synthesized APO is an efficient antioxidant for NBR as IPPD. In comparison with all samples, the NBR compound containing 1 phr of APO has the highest retention rate of tensile strength and elongation at break over the entire period.

Thermal study

The thermal stability of the prepared NBR compounds with 1 phr of commercial antioxidant (IPPD) and 1 phr of APO is investigated using thermogravimetric analysis (TGA) and differential thermogravimetric analysis (DTG). The obtained data

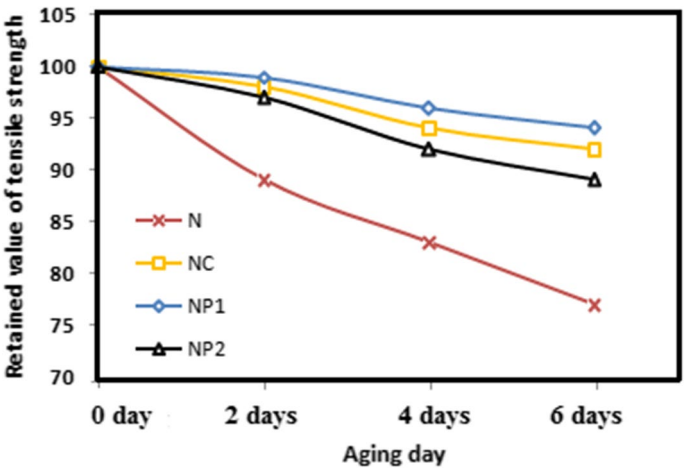

Fig. 5 Retained tensile strength of the prepared NBR compounds after 2, 4, and 6 days of thermal aging

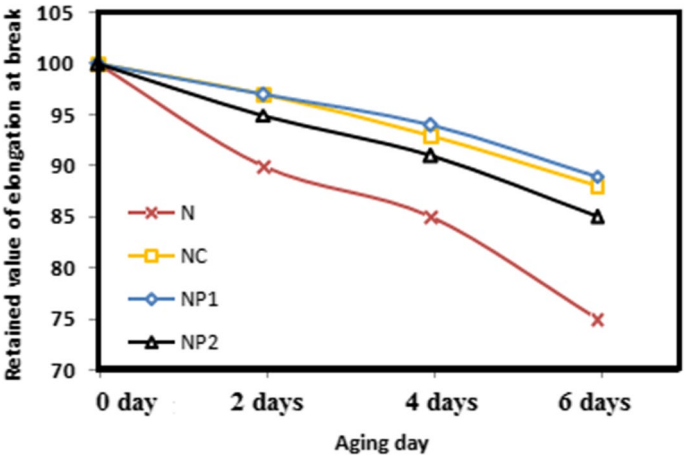

Fig. 6 Retained elongation at break (%) of the prepared NBR compounds after 2, 4, and 6 days of thermal aging

are shown in Fig. 7. As observed, the two NBR compounds exhibit a single-stage decomposition (364–552 °C), which is due to the decomposition of NBR segments. It is also noted that the TGA curve of the NBR compound with APO has a small upward shift to a temperature of 461 °C compared to that with IPPD (452 °C). This indicates that the NBR compound with APO is more thermally stable than the compound with IPPD. This stability arises from the presence of more cross-links within compound with APO than that with IPPD as revealed by the cross-link density results.

Dielectric and conductivity measurements

The real (ε') and imaginary (ε'') components of the relative dielectric permittivity, loss factor (tanδ), and conductivity (σ) versus frequency (f) of NBR/SiO_2

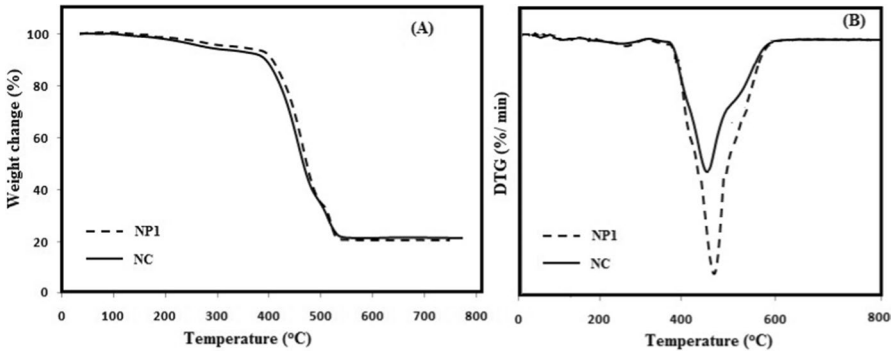

Fig. 7 TGA **A** and DTG **B** of NBR compounds with 1 phr of IPPD antioxidant (NC) and 1 phr of APO (NP1)

compounds are presented in Fig. 8. The results in Fig. 8 demonstrate the significant impact of the commercial IPPD and the prepared APO chemical structure on the investigated NBR/SiO_2 compounds. As seen from the figure, the values of permittivity ε', dielectric loss ε'', loss factor tanδ and conductivity σ of NBR/SiO_2 compounds containing IPPD are higher compared to those of compounds containing the prepared APO. This decrease can be related to the formation of hydrogen bond between the –NH– groups of APO and the –CN groups of NBR [21]. Further, silanol group of SiO_2 which are highly polar groups [22], are reduced, along with the quantity of charge carriers via interfacial interaction and hydrogen bonds among SiO_2 and the molecular chains of NBR [23]. However, these factors show a descending trend by increasing APO concentration. This pattern is further supported by the results demonstrated in Fig. 9 at fixed frequency (100 Hz) for comparison, which clearly shows that the inherent variation in the used matrix antioxidant is mostly responsible for the diversity in the NBR/SiO_2 compounds' dielectric characteristics.

In addition, the sharp rise of ε' and ε'' values detected in all samples at low frequencies are due to the accumulation of free charges at the interface between the material and electrodes. Principally, the total polarization enhances in multi-component materials as a result of interfacial polarization effects [24, 25].

Furthermore, the construction of a three-dimensional network of the particles within the rubber matrix may be the cause of the electrical conductivity of compound materials. Two mechanisms are known to be in charge of the electrical performance of filled rubbers [26]. The first mechanism happens when particles

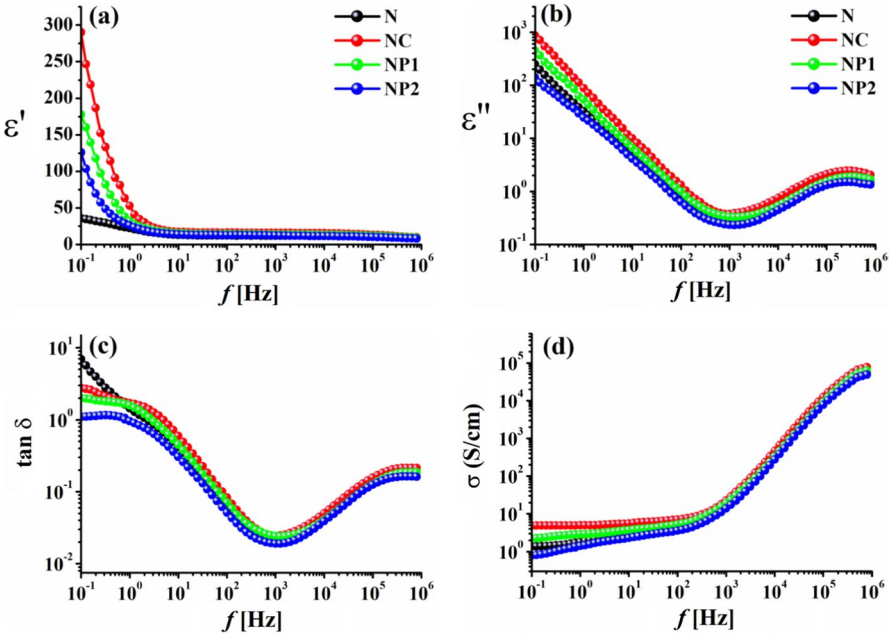

Fig. 8 The permittivity (ε'), dielectric loss (ε''), loss factor (tanδ) and conductivity (σ) as a function of frequency (f) for NBR/SiO_2 compounds, at 30 °C, respectively

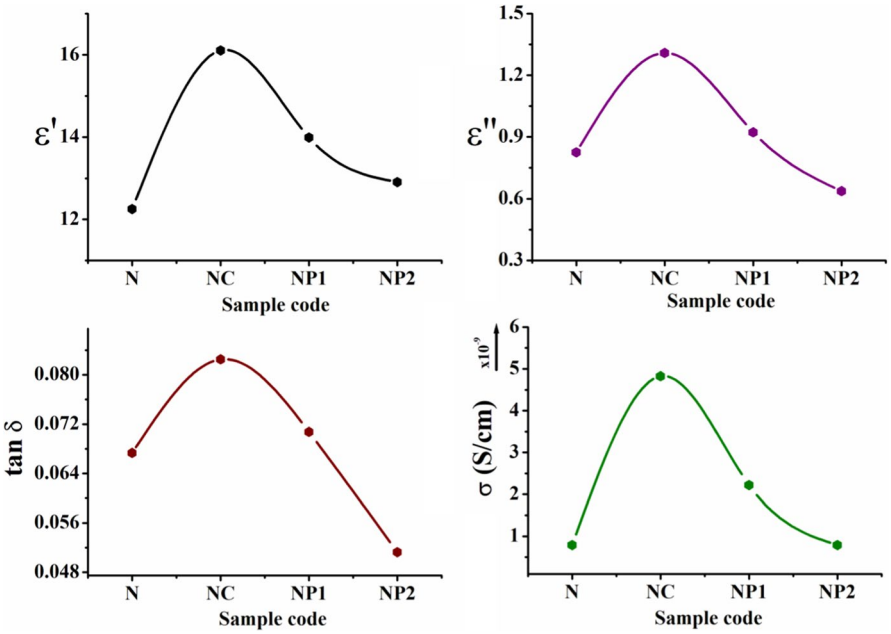

Fig. 9 **a–c** Dependence of the permittivity ε', dielectric loss ε'' and loss tangent tanδ on sample composition at fixed frequency (100 Hz). **d** Variation of conductivity σ with sample composition

come into direct touch with one another and carriers can move from one particle to another [27]. The second process is the so-called tunnel effect [28], which happens when two particles are separated by a thin rubber insulating barrier. The insulating rubber barrier between the particles prevents contact between them, yet electron transport is still feasible. However, the electrons can jump from one particle to another when the potential difference reaches a particular level. These mechanisms can only be activated if the rubber matrix has a filler network. The existence or absence of filler network is influenced by a number of factors, such as their concentration, size and other particle-specific characteristics. If the filler concentration is sufficient to form a network, along with the foregoing, the polarity of the IPPD system also plays a dominant role in enhancing the compound conductivity and helps to explain the effects seen in the compounds under study [29].

The interfacial polarization and ionic conductivity contributions have a significant impact on the dielectric relaxation processes at lower frequencies. Many authors describe the relaxation of the dipole without the effects of conductivity, using the electrical modulus formalism to eliminate these interferences [30–32]. Figure 10a illustrates the frequency dependence of the real component of electric modulus (M') of NBR/SiO_2 compounds. According to observations made at low frequencies, M' for all compounds approaches zero, which suggests that electrode polarisation has little effect [31, 33]. On the other hand, M' has a maximum value at higher frequencies. The conductivity relaxation process may be the cause of the dispersion between

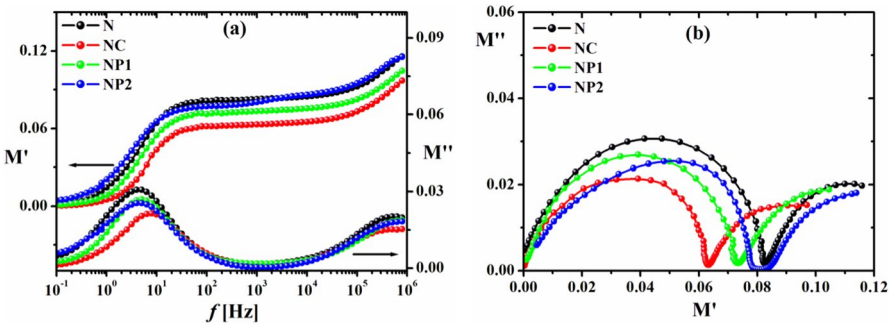

Fig. 10 **a** The real and imaginary parts of electric modulus (M' & M'') versus frequency (f) for NBR/SiO_2 compounds, at 30 °C, respectively. **b** Cole–Cole plots of M'' versus M' for NBR/SiO_2 compounds

these frequencies [34]. The short-range mobility of charge carriers may be the cause of a continuous dispersion on rising frequency [32, 35].

Adittionaly, Fig. 10a depicts the variation of the imaginary component of the electric modulus (M'') as a function of frequency. A main relaxation peak present in the plots of this figure at lower frequency. As APO loading is increased, the peak maximummoves toward a higher frequency. The non-Debye type of relaxation in the material is supported by the observed asymmetry in peak broadening, which reveals a spread of relaxation times [36].

Figure 10b represents Cole–Cole or Nyquist plots of NBR/SiO_2 compounds. In the Cole–Cole plots, there were two main arcs. The left side semicircle is the first one, which is related to lower frequency relaxation and is a result of interfacial polarization [37, 38], whereas the other one is associated to the α-relaxation due to the main chain motions [39–41]. As seen in this figure, the semicircles' nature altered clearly by adding IPPD and APO as shown by the variations in the semicircle's radius. This implies that the relaxation mechanisms are influenced by their incorporation. Additionally, the start of semicircles coincides with the graph's origin, which is a clear sign that no additional relaxing process is existed.

The Nyquis plots of NBR/SiO_2 compounds presented in Fig. 10b facilitate exploring the nature of the relaxation mechanisms, which are present at both low and high frequencies. On the later bases, multi-peak fitting method is used to fit the curves of M'' versus f in Fig. 10a by utilizing a computer program based on the Havriliak–Negami functions which has been extensively used to describe the relaxation behavior of polymeric systems [31]. Two dielectric relaxations are present in all samples after M'' analysis (Fig. 11). They are referred to interfacial polarization and the α-relaxation due to the main chain motions as discussed earlier in Fig. 10b. From the fitting results of Fig. 12, it is seen that the maximum of the relaxation peak I (f_{max}) of IPPD (NC) shifts to higher frequencies which referred to the increase of conductivity of the sample, whereas the shift of peak (II) attributed to change in the degree of cross-linking [40]. However, the shift of the f_{max} of peak (II) to lower frequency increased after addition of APO (NP1) which could be attributed to the reduction of the segmental mobilities as a result of some sort of interactions

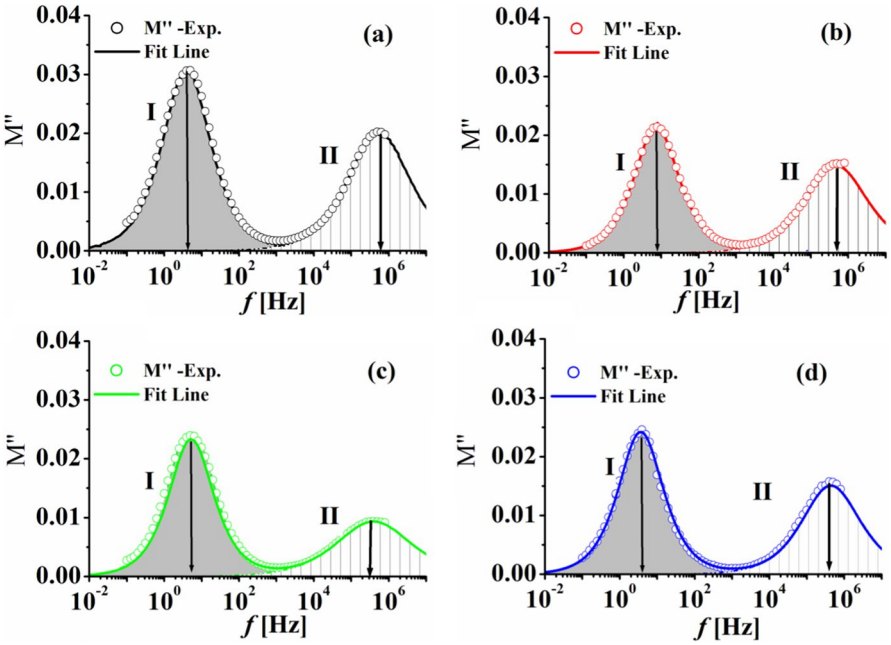

Fig. 11 Analyses of NBR/SiO_2compounds. Samples code are: (**a** N, **b** NC, **c** NP1, **d** NP2)

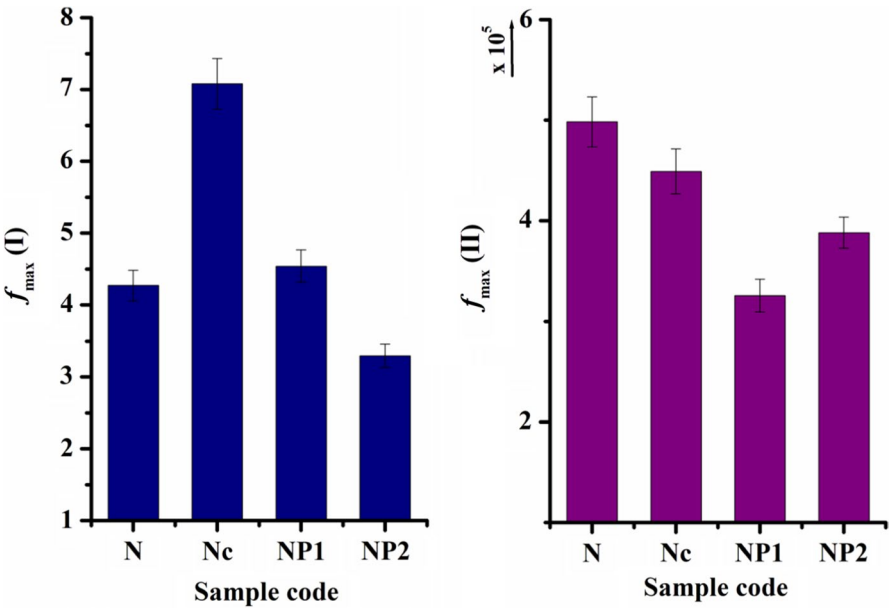

Fig. 12 Dependence of the position of f_{max} of relaxation peaks I and II on sample composition

between -CN groups of NBR and amino groups in APO. These finding are in line with the results in Fig. 8.

Conclusion

This study explores the impact of incorporating APO as antioxidant for NBR compounds on their cure, mechanical, swelling, anti-aging, thermal and dielectric properties. Two different concentrations of APO (1 & 2 phr) are used. The obtained results demonstrate that the APO exerts a relatively slight effect on cure properties of NBR compounds. However, the most notable improvements were observed in swelling, mechanical, and thermal properties when 1 phr of it is used compared to the blank NBR compound (without any antioxidant) while its effect is approximately close to that prepared with a commercial antioxidant; IPPD. These findings, along with the retained values of mechanical properties that are almost close to commercial IPPD, demonstrate that the prepared APO performs comparably to the commercial alternative. This similarity, when coupled with its superior mechanical and thermal attributes, establishes it as a well-rounded choice for long-lasting rubber applications.

Additionally, the NBR compounds with APO show lower dielectric properties (conductivity and permittivity) compared to that prepared with commercial one making them preferable in applications requiring electrical insulation and resistance as power distribution systems, and capacitor manufacturing.

References

1. Yasin T, Ahmed S, Yoshii F (2002) Radiation vulcanization of acrylonitrile–butadiene rubber with polyfunctional monomers. React Funct Polym 53:173–181. https://doi.org/10.1016/S1381-5148(02)00171-2
2. Jeon SK, Kwon OH, Tak NH, Chung NK, Baek UB, Nahm SH (2022) Relationships between properties and rapid gas decompression (RGD) resistance of various filled nitrile butadiene rubber vulcanizates under high-pressure hydrogen. Mater Today Commun 30:103038–103047
3. Li B, Sh-x Li, Shen M-x, Xiao Y-l, Zhang J, Xiong G-y, Zhang Z-n (2021) Tribological behaviour of acrylonitrile–butadiene rubber under thermal oxidation ageing. Polym Test 93:106954–106965
4. Moon SCh, Jo BW, Farris RJ (2009) Flame resistance and foaming properties of NBR compounds with halogen-free flame retardants. Polym Compos 30:1732–1742
5. Wang Q (2014) The thermal resistance, flame retardance, an smoke control mechanism of nano MH/GF/NBR composite material. Sci Eng Compos Mater 21:309–3014
6. Ghamarpoor R, Jamshidi M (2022) Preparation of superhydrophobic/superoleophilic nitrile rubber (NBR) nanocomposites contained silanized nano silica for efficient oil/water separation. Sep Purif Technol 291:120854
7. Zhong R, Zhang Z, Zhao H, He X, Wang X, Zhang R (2018) Improving thermo-oxidative stability of nitrile rubber composites by functional graphene oxide. Materials 11:921–935
8. Ahmed FS, Shafy M, Abd El-megeed AA, Hegazi EM (2012) The effect of γ-irradiation on acrylonitrile–butadiene rubber NBR seal materials with different antioxidants. Mater Des 1980–2015 36:823–828
9. Abad LV, Relleve LS, Aranill CT (2002) Natural antioxidants for radiation vulcanization of natural rubber latex. Polym Degrad Stab 76:275–279

10. Kandil H, Nashar DE, Ward AA, Khalaf AI (2022) Jojoba seed powder as eco-friendly antioxidant for rubber products. J Appl Polym Sci 139:e52642–e52652
11. Wu W, Zeng X, Li H, Lai X, Xie H (2015) Synthesis and antioxidative properties in natural rubber of novel macromolecular hindered phenol antioxidants containing thioether and urethane groups. Polym Degrad Stab 111:232–238
12. Zidan TA, El-Sabbagh SH, Yehia AA (2022) Synthesis and evaluation of methyl 3, 4, 5-trihydroxybenzoate and methyl 3, 4, 5-trihydroxybenzohydrazide as additives for natural rubber composites. Egypt J Chem 65:531–538
13. Zidan TA (2023) Rhodanine-chitosan hydrogel as a novel antioxidant for acrylonitrile–butadiene rubber composites. J Vinyl Addit Technol. https://doi.org/10.1002/vnl.22053
14. Mayer J, Metzsch-Zilligen E, Pfaendner R (2022) Novel multifunctional antioxidants for polymers using eugenol as biogenic building block. Polym Degrad Stab 200:109954
15. Bergenudd H, Eriksson P, Armitt CD, Stenberg B, Jonsson EM (2002) Synthesis and evaluation of hyperbranched phenolic antioxidants of three different generations. Polym Degrad Stab 76:503–509
16. Li C, Sun P, Wang H, Ma L, Kang W, Zhang Z, Wang J (2017) Synthesis and oxidative stability of hyperbranched macromolecule-bridged hindered phenols. New J Chem 41:6395–6404
17. Zidan TA, Youssef AM, El-Menyawy EM, Kandil HS (2021) A new star-shaped amino functionalized poly(phenylene oxide) for optoelectronic applications. Polym Sci Ser B 63:781–789
18. Kandil H, Abo-Salem HM (2023) A novel thiourea based interfacial modifier for silica-filled natural rubber composites. J Appl Polym Sci 140:e53550
19. Surya I, Hayeemasae N, Ginting M (2018) In: IOP conference series: materials science and engineering. Vol 343, p 012009. IOP Publishing
20. Spanheimer V, Katrakova-Krüger D, Altenhofer P, Valtchev K (2023) Evaluation of the suitability of different methods for determination of the crosslink density in highly filled EPDM compounds. J Polym Res 30:24
21. Song M, Wang X, Wu S, Qin Q, Yu G, Liu Z, Pei H, Zhang Y, Jiao M (2022) How the hindered amines affect the microstructure and mechanical properties of nitrile-butadiene rubber composites. E-Polymers 20:8–15
22. Ward AA, Bernhard S, Wolfgang VS, Stephan H, Augenie MB, Faika FH (2003) Studies on the dielectric behavior of silica-filled butyl rubber vulcanizates after cyclic deformation. J Macromol Sci Phys 42:1265–1280
23. Liu X, Zhou X, Kuang F, Zuo H, Huang J (2021) Mechanical and tribological properties of nitrile rubber reinforced by nano-SiO_2: molecular dynamics simulation. Tribol Lett 69:54
24. Malas A, Bharati A, Verkinderen O, Goderis B, Moldenaers P, Cardinaels R (2017) Effect of the GO reduction method on the dielectric properties, electrical conductivity and crystalline behavior of PEO/rGO nanocomposites. Polymers 9:613–633
25. Hafez RS, Hakeem NA, Ward AA, Ismail AM, Abd El-kader FH (2020) Dielectric and thermal properties of PEO/PVDF blend doped with different concentrations of $Li_4Ti_5O_{12}$ nanoparticles. J Inorg Organomet Polym 30:4468–4480
26. Gojny FH, Wichmann MH, Fiedler B et al (2006) Evaluation and identification of electrical and thermal conduction mechanisms in carbon nanotube/epoxy composites. Polymer 47:2036–2045
27. Kandil H, Youssef AM, El Nashar DE (2022) Lignin as a dry bonding system component in EPDM/microcrystalline cellulose composites. J Appl Polym Sci 139(6):51616–51626
28. Li C, Tostenson ET, Chou TW (2007) Dominant role of tunneling resistance in the electrical conductivity of carbon nanotube–based composites. Appl Phys Lett 91:223114
29. Schauser NS, Grzetic DJ, Tabassum T, Kliegle GA et al (2020) The role of backbone polarity on aggregation and conduction of ions in polymer electrolytes. Am Chem Soc 142:7055–7065
30. Mohomed K, Moussy F, Harmon JP (2006) Dielectric analyses of a series of poly(2-hydroxyethyl methacrylate-co-2,3-dihydroxypropyl methacylate) copolymers. Polymer 47:3856–3865
31. Abdel-Aal SK, Hassan ML, Abou Elseoud WS, Ward A (2022) High-lignin-content rice straw cellulose nanofibers/graphene oxide nanocomposites films: electrical and mechanical properties. J Appl Polym Sci 139:e53107–e53118
32. Moustafa AM, Gad SA, Ward AA (2021) Impact of molybdenum doping on the structural, optical and dielectric properties of α-Al_2−x $MoxO_3$. ECS J Solid State Sci Technol 10:043007
33. Chatterjee B, Gupta PN (2012) Nanocomposite films dispersed with silica nanoparticles extracted from earthworm humus. J Non-Cryst Solids 358:3355–3364
34. Dutta A, Sinha TP, Jena P, Adak S (2008) Ac conductivity and dielectric relaxation inionically conducting soda-ime-silicate glasses. J Non-Cryst Solids 354:3952–3957

35. Behera B, Nayak P, Choudhary RNP (2007) Study of complex impedance spectroscopic properties of $LiBa_2Nb_5O_{15}$ ceramics. Mater Chem Phys 106:193–197
36. Kaur B, Singh L, Reddy VA, Jeong DY, Dabra N, Hundal JS (2016) AC impedance spectroscopy, conductivity and optical studies of Sr doped bismuth ferrite nanocomposites. Int J Electrochem Sci 11:4120–4135
37. Dang TTN, Mahapatra SP, Sridhar V, Kim JK, Kim KJ, Kwak H (2009) Dielectric properties of nanotube reinforced butyl elastomer composites. J Appl Polym Sci 113:1690–1700
38. Sun H, Zhang H, Liu S, Ning N, Zhang L, Tian M, Wang Y (2018) Interfacial polarization and dielectric properties of aligned carbon nanotubes/polymer composites: the role of molecular polarity. Compos Sci Technol 154(18):145–153
39. Utrera-Barrios S, Manzanares RV, Araujo-Morera J, González S, Verdejo R, López-Manchado MÁ, Santana MH (2021) Understanding the molecular dynamics of dual crosslinked networks by dielectric spectroscopy. Polymers 13:3234–3254
40. Adachi H, Adachi K, Aka T (1980) Effects of cross-linking density and of stretching on dielectric in poly(acrylonitrile-co-butadiene) rubber. Polym J 12:329–334
41. Hedvig P (1977) Dielectric spectroscopy of polymers. Akademiai Kiado, Budapest, p 312